Theoretical Analysis of Microtubule Dynamics at All Times

Xin Li and Anatoly B. Kolomeisky*

Rice University, Department of Chemistry and Center for Theoretical Biological Physics, Houston, TX 77005

E-mail: tolya@rice.edu

Phone: +1 713 3485672. Fax: +1 713 3485155

*To whom correspondence should be addressed

Abstract

Microtubules are biopolymers consisting of tubulin dimer subunits. As a major component of cytoskeleton they are essential for supporting most important cellular processes such as cell division, signaling, intracellular transport and cell locomotion. The hydrolysis of guanosine triphosphate (GTP) molecules attached to each tubulin subunit supports the nonequilibrium nature of microtubule dynamics. One of the most spectacular properties of microtubules is their dynamic instability when their growth from continuous attachment of tubulin dimers stochastically alternates with periods of shrinking. Despite the critical importance of this process to all cellular activities, its mechanism remains not fully understood. We investigated theoretically microtubule dynamics at all times by analyzing explicitly temporal evolution of various length clusters of unhydrolyzed subunits. It is found that the dynamic behavior of microtubules depends strongly on initial conditions. Our theoretical findings provide a microscopic explanation for recent experiments which found that the frequency of catastrophes increases with the lifetime of microtubules. It is argued that most growing microtubule configurations cannot transit in one step into a shrinking state, leading to a complex overall temporal behavior. Theoretical calculations combined with Monte Carlo computer simulations are also directly compared with experimental observations, and the good agreement is found.

keywords: cytoskeleton proteins, dynamic instability, aging, dynamic processes

INTRODUCTION

The cytoskeleton network in biological cells is composed of microtubules, actin filaments and intermediate filaments.[1] Both microtubules and actin filaments are active polymers which play a central role in many fundamental cell activities, such as mechanical stability of cells, cell division, signaling and cell motility.[2,3] The dynamic process of self-assembly for microtubules and actin filaments are driven by the hydrolysis of GTP (guanosine triphosphate) or ATP (adhenosine triphospate) molecules bound to each subunit along the filaments. Microtubules can be viewed as polar polymers with one end (called "minus") mostly localized in the central part of the cell and with a "plus" end growing freely closer to the boundaries of the cell. One of the most intriguing properties of microtubules is the phenomenon of dynamic instability, which turned out to be critically important for many biological processes.[4,5] During the assembly of microtubules the growth phase is often stochastically interrupted by transition into a rapid shrinking phase, which is known as a catastrophe event. Oppositely, the rapid shrinking of microtubules can also stochastically reverse back into the growing state. This is called a rescue process.[5]

Recently, the catastrophe and rescue events have been observed in both *in vivo* and *in vitro* experiments with very high temporal and spatial resolutions.[6,7] A GTP-cap model has been proposed to explain the dynamic instability in microtubules.[8,9] The growth of microtubules is believed to be protected by a cap composed of unhydrolyzed subunits at the tip of the biopolymer. While the system becomes unstable via stochastic events that include hydrolysis and dissociations of unhydrolyzed subunits, the catastrophe events appear once the GTP-cap is lost. Microtubules can also be rescued from the rapid shrinking or the catastrophe phase when a buried island of unhydrolyzed subunits in the microtubules is exposed during the rapid dissociation of subunits.[10] It slows down the depolymerization and the system might transit back into the growing phase. This picture is quite useful and capable to explain many phenomena observed in experiments. However, a detailed microscopic mechanism of dynamic instability in microtubules remains unclear and many issues are still unresolved.

One of the problems associated with understanding microtubule dynamics is that most theoreti-

cal and experimental studies assume that catastrophes in microtubules are one-step processes.[2,3,8,11,12] Another issue is that even more detailed theoretical investigations concentrate mostly on stationary-state behavior of the system.[13–16] In other words, dynamic properties of microtubules are assumed to be stationary and independent of the time. However, these theoretical views have been challenged recently by high-resolution measurements of filament length and lifetime distributions.[17–20] In these experiments, deviations from exponential distributions expected for the single-transition picture have been observed.[19,20] In addition, it was found that dynamic properties of microtubules change with time.[17,19,20] Furthermore, experiments show that various types of kinesin motor proteins bound to microtubules might influence these aging phenomena differently.[19,20] These observations raise several fundamental questions including what are the microscopic mechanisms of aging in microtubule dynamics, and if the stationary-state behavior can be achieved. However, there are very few theoretical studies on age-dependent phenomena in microtubules.[20]

Our goal is to develop a theoretical framework for understanding aging phenomena in microtubule dynamics. In this article we focus on investigating the temporal evolution of microtubule assembly by analyzing the time-dependent distributions of clusters of unhydrolyzed subunits along the microtubules. A similar model was proposed recently by us,[16] however, only stationary-state properties of the system have been discussed. Our calculations show how the temporal evolution of microtubules can be evaluated from the analysis of dynamics of the cluster distributions. The dynamic behavior of the system is found to be influenced by the initial conditions. Therefore, we considered the microtubule assembly by varying the initial conditions. It is shown that the simple theoretical model proposed here is able to explain the aging observed in recent experiments. Another advantage of our method is that it provides a microscopic picture for these complex phenomena. We suggest that transitions from polymer configurations in the growing phase to configurations in the shrinking phase in most cases cannot take place directly but should go through the intermediate states, leading to a complex temporal dependence of the microtubule dynamic properties.

THEORETICAL METHOD

Our idea is to employ a discrete-state stochastic approach[15,16,21] that takes into account most relevant chemical transitions in the system. It is also a very convenient method since analytical calculations can be done, providing a large amount of microscopic information on complex processes during the microtubule assembly. The microtubule is a cylindrical tube that typically consists of thirteen parallel protofilaments.[2,3] We consider a simplified single-filament model, as shown in Fig.1, to describe the system. This approach has been successfully applied to characterize various properties of the microtubule assembly.[15,16,21] The "minus" end of microtubules is usually fixed in *in vitro* experiments, as illustrated in Fig. 1, or it is located at the specific position in the center of the cell, so only the "plus" end is free to grow or exchange subunits between filaments and the solution. Because of this observation, we focus on dynamics of the microtubule assembly of the "plus" end only. The tubulin dimers bound with GTP molecules can attach to or detach from the "plus" end of the microtubules with rates U and W_T, respectively (see Fig. 1). The GTP molecules bound to the subunits might be transformed into GDP (guanosine diphosphate) and Pi (phosphate) through the hydrolysis process after tubulin dimers are incorporated into the microtubules. The GTP hydrolysis is a multi-step process which includes a fast GTP cleavage and a slow Pi release. We will consider here a simplified two-state picture to describe a chemical state of each monomer in the microtubule. It assumes that each subunit either contains the unhydrolyzed GTP (T-subunit) or it is bound to the hydrolyzed GDP molecule (D-subunit): see Fig. 1.[15,21] The hydrolysis mechanism for the cytoskeleton filament is still under discussion,[21–30] and we assume here that all T-subunits on microtubules can be hydrolyzed with the same rate r as indicated in Fig.1. The hydrolyzed D-subunits can detach from the "plus" end of the microtubules with a rate W_D (see Fig. 1).

We assume in our model that the attachment rates are proportional to the amount of free tubulin molecules in the solution, $U = k_{on}C_T$, where k_{on} is a rate constant and C_T is a concentration of free T-subunits. The detachment rates W_T and W_D for T- and D-subunits, correspondingly, generally have different values. But to explain our method better we first consider a special case when

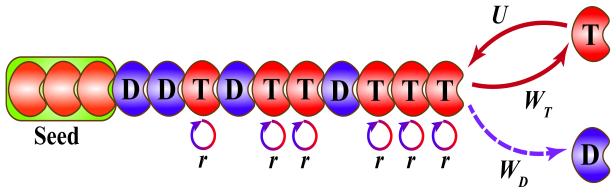

Figure 1: A schematic view of the microtubule assembly process in a single-filament model. The tubulin dimers bound with GTP molecules are labeled as T-subunits in red color, while those bound with GDP molecules are labeled as D-subunits in blue color. The "minus" end of the microtubule is fixed and the microtubule grows at the "plus" end from a seed. The attachment and detachment rates of the T-subunits at the "plus" end of microtubules are given by U and W_T, respectively. W_D is the detachment rate for D-subunits. All T-subunits along the microtubule can be hydrolyzed with the same rate r.

these detachment rates are equal, $W_T = W_D$, since the analytical solution can be obtained for this situation. Then, the general case of $W_T \neq W_D$ will be discussed later in the paper.

To study the dynamics of microtubule assembly, the cluster distribution functions $S_n(l,t)$ were introduced in previous studies.[16] They are defined as the probabilities to detect a cluster of size l (consisting of all unhydrolyzed T-subunits) starting from the site n (counting from the tip of microtubules) at time t *independently* from the state of all other subunits in the filament. The use of the cluster distributions is important because it allows us to capture significant correlations that are present in this effectively one-dimensional system and affect its dynamics.[16] The temporal evolution of these cluster distributions obviously depends on the initial conditions from which the microtubules start to grow. Therefore, we discuss several various initial conditions, including the microtubules growing from a seed composed of all D- or T-subunits, respectively.

RESULTS AND DISCUSSION

The dynamics of the cluster distribution function $S_n(l,t)$ can be described by a set of Master equations,[16]

$$\frac{dS_n(l,t)}{dt} = US_{n-1}(l,t) + W_T S_{n+1}(l,t)S_1(1,t) + W_D S_{n+1}(l,t)(1-S_1(1,t)) - [U + lr + W_T S_1(1,t) + W_D(1-S_1(1,t))]S_n(l,t). \quad (1)$$

for $n > 1$. This equation can be viewed as a balance of probability fluxes from different cluster configurations. The first three terms on the right side of the Master equation represent positive fluxes into the given cluster state due to adding the tubulin subunit to the biopolymer, and detaching hydrolyzed or unhydrolyzed subunits from it. The last term is the flux out of the given state due to the attachment/detachment of subunits as well as due to the hydrolysis. For the case of equal detachment rates of T- and D-subunits from the filament tip, $W_T = W_D = W$, the general Master equation simplifies into

$$\frac{dS_n(l,t)}{dt} = US_{n-1}(l,t) + WS_{n+1}(l,t) - (U + W + lr)S_n(l,t), \quad (2)$$

The corresponding Master equations to describe the dynamics for the end subunit ($n = 1$) can be written as

$$\frac{dS_1(l,t)}{dt} = US_1(l-1,t) + WS_2(l,t) - (U + W + lr)S_1(l,t), \quad (3)$$

for $l > 1$. At the same time, the temporal evolution of the cluster $S_1(1,t)$ with $n = 1$ and $l = 1$ is given by

$$\frac{dS_1(1,t)}{dt} = U + WS_2(1,t) - (U + W + r)S_1(1,t). \quad (4)$$

To solve these time-dependent equations, we consider Laplace transforms for the cluster distributions, which are defined as

$$\tilde{S}_n(l,s) = \int_0^\infty e^{-st} S_n(l,t)dt. \quad (5)$$

These Master equations are differential equations, so to obtain solutions for the temporal evolution of clusters, $S_n(l,t)$, we need to know the initial conditions. Several sets of initial conditions are considered in this paper as explained below.

Microtubule grows from a seed with all D-subunits

First, we consider the case when the microtubules start to grow from a seed segment that consists of all hydrolyzed D-subunits. This means that

$$S_n(l,t=0)=0, \tag{6}$$

for all $n,l>0$, initially. Then, Eq. (2), Eq. (3) and Eq. (4) in terms of Laplace transforms can be written in the following form,

$$(s+U+W+lr)\tilde{S}_n(l,s)=U\tilde{S}_{n-1}(l,s)+W\tilde{S}_{n+1}(l,s), \quad \text{for } n>1, \tag{7}$$

$$(s+U+W+lr)\tilde{S}_1(l,s)=U\tilde{S}_1(l-1,s)+W\tilde{S}_2(l,s), \quad \text{for } l>1, \tag{8}$$

$$(s+U+W+r)\tilde{S}_1(1,s)=\frac{U}{s}+W\tilde{S}_2(1,s). \tag{9}$$

We are looking for a solution $\tilde{S}_n(l,s)$ of the above equations in the following form,

$$\tilde{S}_n(l,s)=B_l x_l^n, \tag{10}$$

where B_l and x_l are unknown parameters to be determined. By substituting Eq. (10) into Eq. (7), we have

$$Wx_l^2-(s+U+W+lr)x_l+U=0, \tag{11}$$

which leads to

$$x_l=\frac{s+U+W+lr-\sqrt{(s+U+W+lr)^2-4UW}}{2W}. \tag{12}$$

Similarly, the substituting Eq. (10) into Eq. (9) leads us to

$$(s+U+W+r)B_1x_1 = \frac{U}{s} + WB_1x_1^2. \tag{13}$$

Considering $l = 1$ in Eq. (11), we obtain another expression for x_1 which is described by

$$(s+U+W+r)x_1 = U + Wx_1^2. \tag{14}$$

By comparing Eq. (13) and Eq. (14), one can easily derive that

$$B_1 = \frac{1}{s}. \tag{15}$$

Finally, by substituting Eq. (10) into Eq. (8), we obtain the following result,

$$(s+U+W+lr)B_lx_l = UB_{l-1}x_{l-1} + WB_lx_l^2. \tag{16}$$

Combining this relation with Eq. (11), a simple expression for the parameter B_l is produced,

$$B_l = B_{l-1}x_{l-1} = B_1\prod_{k=1}^{l-1} x_k. \tag{17}$$

Therefore, the Laplace transform $\tilde{S}_n(l,s)$ of the cluster distribution function $S_n(l,t)$ can be expressed explicitly by

$$\tilde{S}_n(l,s) = B_lx_l^n = B_1x_l^{n-1}\prod_{k=1}^{l} x_k, \tag{18}$$

where parameters x_l and B_1 are given by Eq. (12) and Eq. (15), respectively.

The knowledge of the functional form for $\tilde{S}_n(l,s)$ allows us to calculate time-dependent cluster distribution functions $S_n(l,t)$ via inverse Laplace transformations. Several examples for clusters of size $l = 1,2$ and 3 at the tip of microtubules [$S_1(1,t)$, $S_1(2,t)$ and $S_1(3,t)$] are presented in Fig. 2 (A) for the parameters listed in Table 1 (except that we use $W_T = W_D = 24$ s^{-1}) and for the free

tubulins concentration $C_T = 9\mu M$. For the microtubule assembly under these initial conditions, the cluster distributions are increasing functions of time and a plateau is reached at the stationary state after a certain time, as shown in Fig. 2 (A). One can see from this Figure that, as expected, smaller clusters reach their steady-state properties faster. Other properties of the system such as the GTP-cap length, the catastrophe frequencies and the rescue times can be also derived from these cluster distribution functions as was explained before.[16]

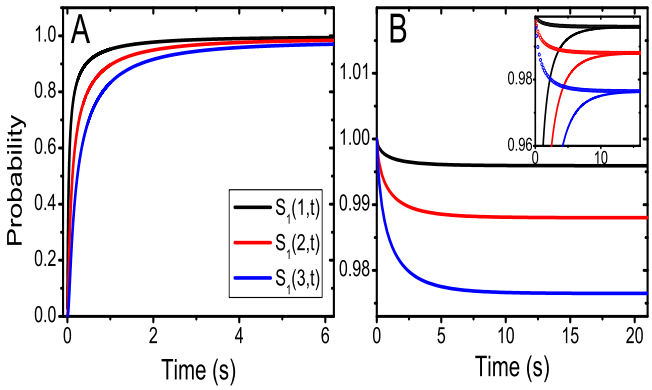

Figure 2: The temporal evolution for cluster distributions $S_1(1,t)$, $S_1(2,t)$, and $S_1(3,t)$ with equal detachment rates $W_T = W_D = 24$ s^{-1}. The cluster distributions are shown for the initial condition that the microtubules grow from a seed composed of (A) all D-subunits, (B) all T-subunits. The free T-subunit concentration is equal to $C_T = 9\mu$M. The inset figure in (B) shows the combination of the main figures (A) and (B) together, indicated by solid and dotted lines, respectively. Other parameter values are listed in Table 1.

Microtubule grows from a seed with all T-subunits

In this section we discuss the case that the microtubules grow from a segment made of all unhydrolyzed T-subunits, i.e., we have

$$S_n(l,t=0) = 1, \tag{19}$$

for all $n, l > 0$. Then, the Laplace transform for Master equations (2)-(4) are given by

$$(s+U+W+lr)\tilde{S}_n(l,s) = 1 + U\tilde{S}_{n-1}(l,s) + W\tilde{S}_{n+1}(l,s), \quad \text{for } n > 1, \tag{20}$$

$$(s+U+W+lr)\tilde{S}_1(l,s) = 1+U\tilde{S}_1(l-1,s)+W\tilde{S}_2(l,s), \text{ for } l>1, \tag{21}$$

$$(s+U+W+r)\tilde{S}_1(1,s) = 1+\frac{U}{s}+W\tilde{S}_2(1,s). \tag{22}$$

Similarly to the previous case, we look for a solution $\tilde{S}_n(l,s)$ of the above equations in the following form,

$$\tilde{S}_n(l,s) = A_l + B_l x_l^n, \tag{23}$$

where A_l, B_l, and x_l again are unknown parameters to be determined from eqs Eq. (20) $\sim$ Eq. (22). Firstly, we substitute the ansatz Eq. (23) into Eq. (20), which gives us

$$(s+U+W+lr)(A_l+B_l x_l^n) = 1+U(A_l+B_l x_l^{n-1})+W(A_l+B_l x_l^{n+1}). \tag{24}$$

Simply changing n by $n-1$ in the above equation leads us to

$$(s+U+W+lr)(A_l+B_l x_l^{n-1}) = 1+U(A_l+B_l x_l^{n-2})+W(A_l+B_l x_l^{n}). \tag{25}$$

Then, we can easily obtain,

$$Wx_l^2-(s+U+W+lr)x_l+U=0, \tag{26}$$

by comparing of Eqs. (24) and (25). The expression above is exactly the same as Eq. (11). Therefore, the explicit formula for x_l can be described by Eq. (12). The parameter A_l is derived from Eqs. (24) and (26), yielding

$$A_l = \frac{1}{s+lr}. \tag{27}$$

By substituting the ansatz Eq. (23) into Eq. (22) leads us to

$$(s+U+W+r)(A_1+B_1x_1) = 1+\frac{U}{s}+W(A_1+B_1x_1^2). \tag{28}$$

Combining with Eq. (27), it can be shown that

$$(s+U+r)A_1 = 1 + \frac{U}{s} - B_1 U, \tag{29}$$

where the parameter A_1 is known from Eq. (27),

$$A_1 = \frac{1}{s+r}. \tag{30}$$

Therefore, the parameter B_1 is given by

$$B_1 = \frac{r}{s(s+r)}. \tag{31}$$

Similarly, by substituting the ansatz Eq. (23) into Eq. (21) and comparing with Eq. (26), we can derive the expression for the parameter B_l. It can be written as

$$B_l = B_1 \prod_{k=1}^{l-1} x_k + \sum_{k=2}^{l-1} \frac{r \prod_{j=k}^{l-1} x_j}{[s+(k-1)r](s+kr)} + \frac{r}{[s+(l-1)r](s+lr)}. \tag{32}$$

The final expression for the Laplace transform $\tilde{S}_n(l,s)$ of the cluster distribution function can be easily obtained from Eq. (23) since all parameters A_l, B_l and x_l are known.

As before, the inverse Laplace transformation of the functions $\tilde{S}_n(l,s)$ allows us to evaluate the cluster distribution functions $S_n(l,t)$ at all times. In Fig. 2(B) we present temporal evolution of clusters of size $l = 1,2$ and 3 at the tip of microtubules [$S_1(1,t)$, $S_1(2,t)$ and $S_1(3,t)$] for the parameters listed in Table 1 (except that we use $W_T = W_D = 24$ s^{-1}) and for the free tubulins concentration $C_T = 9\mu M$. In contrast to the microtubule growth from the seed with D-subunits, these cluster distributions are now decreasing functions of time. A saturation behavior is also observed for these cluster distribution functions after the system reaches the stationary state at a certain time. Again, smaller clusters reach their stationary dynamics faster. In addition, as shown in the inset in Fig. 2(B), the properties of the system at the stationary state are independent of the

initial conditions so curves for cluster distribution functions at different initial conditions coincide at large times. Similar approach can be used to compute temporal evolution of clusters for any initial conditions.

Table 1: Parameters utilized in calculations and the corresponding references.

Parameters	Rates	References
k_{on}, on-rate of T-tubulin dimers (plus end)	3.2 μM^{-1} s^{-1}	Ref.[2]
W_T, off-rate of T-tubulin dimers (plus end)	24 s^{-1}	Ref.[31]
W_D, off-rate of D-tubulin dimers (plus end)	290 s^{-1}	Ref.[2]
r, hydrolysis rate	0.02 s^{-1}	

The knowledge of time-dependent cluster distribution functions $S_n(l,t)$ allows us to estimate *all* dynamic properties of microtubules including frequency of catastrophes, rescue times, GTP-cap size and many others.[16] Recent experiments[19] found that the frequency of catastrophes increases with time. Let us analyze the time dependence of catastrophes. Our theoretical approach explicitly accounts for all polymer configurations in microtubules. As we discussed before,[15,16,21] to calculate the frequency of catastrophes, $f_c(t)$, we need to understand what polymer configurations belong to the growing dynamic phase, and what correspond to the shrinking phase. Then the frequency of catastrophes is equal to the total rate out of the growing phase into the shrinking phase. We define the growing state of the microtubules as all polymer configurations with the GTP-cap of nonzero size, and also the configurations where the number of GDP-subunits at the tip is less than N.[15] All other configurations of the microtubule are considered to be in the shrinking phase. The parameter N has an important physical meaning. It gives the chemical composition of the tip of the microtubule in configurations that show sustained length shortening. For the simplest case of $N = 1$, the catastrophe frequency $f_c(t)$ is given by

$$f_c(t) = r + W_T\,[1 - S_1(2,t)/S_1(1,t)]\,. \tag{33}$$

The first term on the right-hand side of this equation comes from the hydrolysis of the T-subunit at the tip of the microtubule, and the second term is given by the detachment of the unhydrolyzed

T-subunit at the tip which exposures the succeeding hydrolyzed D-subunit. For other cases with $N > 1$ the analytical expressions for the catastrophe frequency can also be obtained as shown in previous studies.[15] The important observation here is that the frequency of catastrophes is always fully determined by the transition rates and by the cluster distribution functions. Since $S_n(l,t)$ can be evaluated for any initial conditions, as explained above, we can calculate the time dependence of the catastrophe frequency.

In Fig. 3 we present several examples of how the catastrophe frequencies change with time for the parameters listed in Table 1 (except that we use $W_T = W_D = 24$ s^{-1}) and for the free tubulins concentration $C_T = 9\mu M$. For the microtubule growth process starting from the fully hydrolyzed seed, $f_c(t)$ is very high at early times but then it decreases as a function of time until the system reaches the stationary state where the catastrophe frequency becomes the time-independent quantity (see Fig. 3). The behavior is different for the situation when the seed consists of only T-subunits. The catastrophe frequency is close to zero as the microtubules start to grow, then it begins to increase as a function of time until the stationary state is approached and the catastrophe frequency becomes independent of the time (Fig. 3). As expected, the stationary-state dynamics of $f_c(t)$ is independent of the initial conditions. These observations can be easily explained using following arguments. As the microtubule starts from a segment with all D-subunits there is no GTP-cap to protect the biopolymer, and it is rather unstable. Then the frequency of catastrophes is expected to be very high at early times. As the microtubule grows the protective cap starts to build up at the tip of the filament, and the biopolymer becomes much more stable. As a result, the frequency of catastrophes decreases. The opposite behavior is expected for the situation when the seed consists of all T-subunits. The catastrophe frequency is very low initially because of very large protective GTP-cap. As time proceeds this cap becomes smaller and the $f_c(t)$ starts to increase, reaching the steady-state values at large times.

To test our theoretical calculations we also performed a series of Monte Carlo computer simulations. The simulation results are indicated by open symbols in Fig. 3, and it can be seen that they perfectly agree with theoretical predictions. Two opposite limiting initial conditions, with all

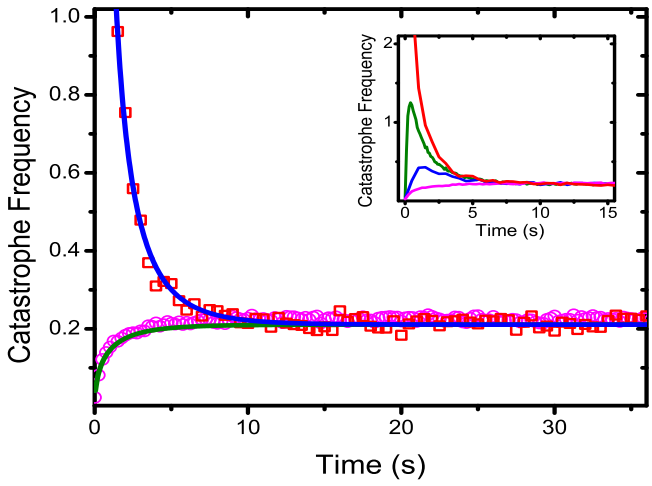

Figure 3: The catastrophe frequency as a function of time with the same parameter values as used in Fig. 2. The blue and green solid lines are obtained from theoretical calculations corresponding to the initial conditions with all D- and all T-subunits, respectively. The open squares and circles are Monte Carlo computer simulations results under initial conditions of all D- and all T-subunits, respectively. The inset figure shows the computer simulation results under variable initial conditions: red line— all D-subunits; green line — all D-subunits except five T-subunits at the tip; blue line — all D-subunits except ten T-subunits at the tip; magenta line — all T-subunits.

D-subunits or with all T-subunits seeds, show very different dynamic behavior, raising the question of what dynamics is expected for seeds with variable chemical composition of hydrolyzed and unhydrolyzed subunits. This problem was investigated using computer simulations, and results are presented in the inset in Fig. 3. We started the microtubule growth from the seeds that had the finite number of T-subunits at the tip followed by all hydrolyzed monomers. The surprising observation is that the frequency of catastrophes shows a non-monotonic behavior with a maximum position at some specific times (see the inset in Fig. 3). The amplitude of the peak becomes smaller as the size of the initial GTP-cap at the tip of the seed segment increases and it will disappear as the size of the GTP-cap becomes large enough. Similarly, if we start from the seeds with the finite number of D-subunits followed by all unhydrolyzed monomers the frequency of catastrophes will go through the minimum. It will be important to test these theoretical predictions in experiments.

Our analysis shows that the frequency of catastrophes increases with time for the processes that start with all T-subunits seeds. It agrees with recent *in vitro* experimental observations.[19] In these

experiments microtubules were growing from the seeds composed of GMPCPP-tubulins, which are essentially the non-hydrolyzable analogs of GTP-tubulins. As we predict, the large protective cap of unhydrolyzed subunits makes $f_c(t)$ much smaller at early times. These observations suggest that aging phenomena in microtubules most probably are associated with non-stationary dynamic behavior and with the approach to the stationary state.

To understand better the temporal evolution of the microtubules growth we also investigated the role of free tubulins in the solution surrounding the filaments. The results are given in Fig. 4 for temporal evolution of catastrophe frequencies for various values of concentrations C_T of free tubulin molecules. Generally, a similar behavior is observed for all concentrations, but increasing C_T lowers the stationary-state values of $f_c(t)$. This result is expected since for large concentrations there is much less possibility for the GTP-cap to fully detach, which lowers the catastrophe frequency.

Our analytical calculations were performed with a simplified assumption that the detachments rates for D- and T-subunits are the same, i.e., $W_T = W_D$. In reality, the hydrolyzed monomers detach much faster (see Table 1). In addition, *in vitro* experiments[19] were done under conditions when no rescues are observed, and the catastrophe times were measured as the the times before the first catastrophe occurs. To make a quantitative test of our theoretical model, we performed Monte Carlo computer simulations for the same experimental conditions with realistic values of the T-subunit attachment rate constants k_{on} and the detachment rate for D-subunits W_D as given in Table 1. The hydrolysis rate r and the detachment rate for T-subunits W_T were varied to get the best fit of experimental measurements. We only recorded the catastrophe time before the catastrophe event appears for the first time as the microtubules grow from the fixed seed made of GMPCPP-tubulins. Then, similarly to experiments, a cumulative distribution of catastrophe times, which gives the fraction of microtubules with catastrophe events taking place before that time, were calculated. We associated the shrinking phase of the microtubules with polymer configurations that have at least

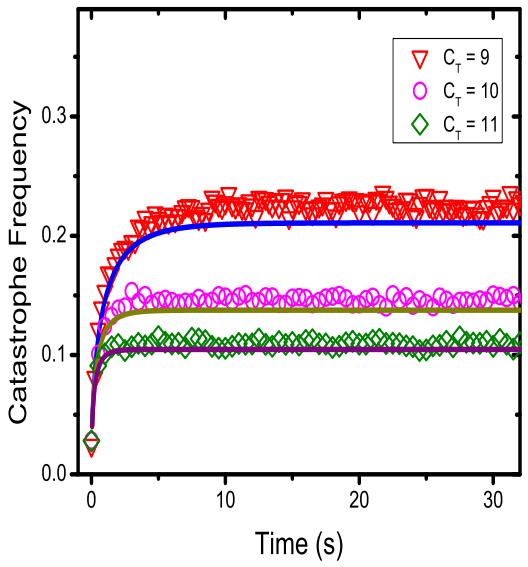

Figure 4: The catastrophe frequency as a function of time for variable concentrations of free tubulin proteins in the solution. The solid lines are obtained from theoretical predictions and the open symbols are calculated from the Monte Carlo computer simulations.

N D-subunits at the end. The parameter N was varied to get the best fit of experimental data. The comparison of computer simulations of our model and experimental results are presented in Fig. 5. It is found that the experimental observations can be well fit by $N = 3$, $W_T = 37.7$ s^{-1}, $r = 0.0036$ s^{-1}, with other parameters as listed in Table 1, and with the free tubulin concentration $C_T = 12\mu M$ as was used in experiments.[19] Our calculations show that $N < 3$ cases cannot describe experimental cumulative distributions. The fact that fitted values are close to experimentally measured values of relevant parameters can be viewed as an additional argument that supports our theoretical picture.

Another advantage of utilizing discrete-state stochastic models for analyzing microtubule dynamics is that this method provides a microscopic explanation for aging phenomena. As illustrated in Fig. 6, we can divide all possible polymer configurations of the microtubule in two dynamic phases, growing or shrinking, depending on the chemical composition of the tip subunits. The frequency of catastrophes corresponds to the total rate out of the growing phase into the shrinking. One can clearly see that for most configurations these transitions cannot take place in one

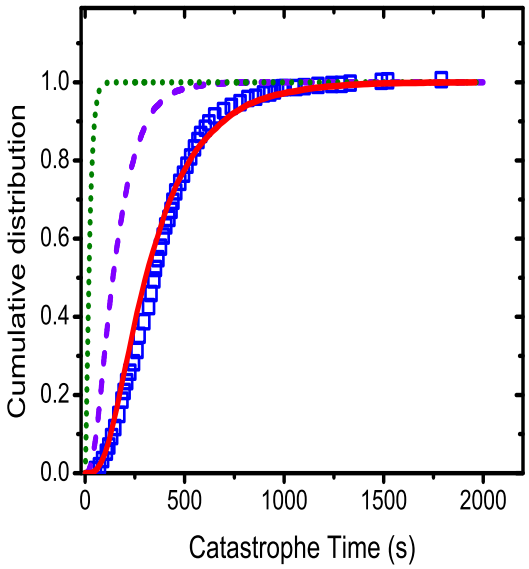

Figure 5: The cumulative distribution of catastrophe times for microtubules. The experimental results are indicated by the blue open squares. The dotted, dashed, and solid lines are obtained from Monte Carlo computer simulations for different choices of N as discussed in the main text. The dotted green line corresponds to $N = 1$, the dashed blue lines describes $N = 2$ case and the solid red line is for $N = 3$.

step. This is the main reason for experimentally observed deviations from the single-transition picture for catastrophes. It also allows us to explain the temporal evolution of the frequency of catastrophes. As time proceeds, the fraction of configurations in the dynamic phase decreases and this should increase the frequency. Similar arguments can be used also to explain the effect of initial conditions on the microtubule dynamics that we found in this work. If the seeds contain all T-subunits then we start with all existing configurations in the growing phase and the rate of catastrophes will increase with the time, as observed in experiments. For the seeds with all D-subunits the situation is different since the system starts with all existing configurations already in the shrinking phase, so the catastrophe rate is large and it will decrease with the time as the system populates more the growing phase: see Fig. 6.

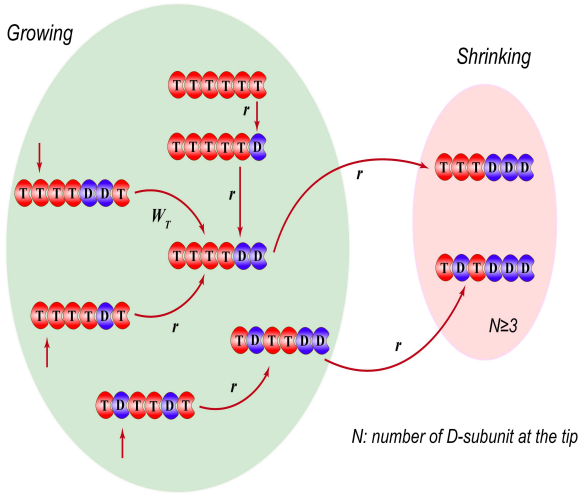

Figure 6: A schematic picture of different polymer configurations for microtubules in the single-filament model. The green oval area contains configurations that belong to the growing dynamic phase, while the pink oval area describes the configurations in the shrinking dynamic phase. Possible transitions between some of the configurations are shown by arrows. Letter symbols describe the corresponding transition rates.

SUMMARY AND CONCLUSIONS

In this paper, we developed a theoretical method for analyzing dynamic properties of microtubules at all times. It is based on discrete-state stochastic models that properly describe all relevant physical-chemical processes in the system. The method computes analytically time-dependent probability distribution functions for subunit clusters of different size and position, which leads to a comprehensive description of all dynamic properties of microtubules. In this work we analyze in detail the frequency of catastrophes at all time scales. Our method is very simple and it allows us to obtain explicitly all dynamic properties. This leads to a better microscopic understanding of complex dynamic processes in microtubules. It is important to note here that our analytical calculations are performed for the special case of equal detachment rates of hydrolyzed and unhydrolyzed subunits. However, based on stationary-state analysis and extensive computer simulations, one might conclude that physical principles of microtubule dynamics are the same even for more realistic conditions.

It is found that the temporal properties of the system are strongly influenced by the initial conditions. For microtubules assembled from seeds consisting of all hydrolyzed D-subunits the cluster distributions of T-subunits are increasing functions of time while decreasing functions are observed when microtubules grow from seeds composed from all unhydrolyzed T-subunits. It leads to a time dependence of all other dynamic properties of microtubules on the initial conditions. More specifically, it is shown that the frequency of catastrophes increases with the time if the process starts from all T-subunits seeds, in agreement with recent *in vitro* experiments. In addition, we found that the process starting from seeds with all hydrolyzed subunits shows a different behavior, with the frequency of catastrophes decreasing with the time. Surprisingly, our method also predicts that for seeds with mixed compositions of T- and D-subunits a non-monotonic temporal dependence of catastrophe frequencies might be observed. This prediction is open for experimental tests. Furthermore, we tested our theoretical calculations with extensive Monte Carlo simulations and excellent agreement is observed for all ranges of parameters. Then we successfully applied the method for analyzing experimental observations on time-dependent dynamics in microtubules. We also pre-

sented microscopic arguments that explain the complex temporal behavior in microtubules and its dependence on the initial conditions. It is argued that dynamics is governed by the relative contributions of polymer configurations in growing and shrinking dynamic phase that change with the time.

Although the developed theoretical method successfully captures the main features of the temporal behavior in microtubule assemblies, as judged by comparing with experiments and extensive Monte Carlo computer simulations, one should remember that the presented approach is rather oversimplified. It ignores many important properties of real microtubules such as multi-filament structures and lateral interactions between the protofilaments. In addition, strictly speaking, our method analytically calculates properties only for the special case when the detachment rates for T- and D-subunits are the same. Although computer simulations and stationary-state calculations show that this assumption does not change the physical principles of these processes, the quantitative details of the time-dependent dynamics in microtubules might be affected. Thus, it will be critically important to test our theoretical predictions in experimental studies in order to determine the applicability and limitations of the method.

Acknowledgement

The work was supported by grants from the Welch Foundation (C-1559), from the NSF (Grant CHE-1360979) and by the Center for Theoretical Biological Physics sponsored by the NSF (Grant PHY-1427654).

References

(1) Alberts, B.; Johnson, A.; Lewis, J.; Raff. M.; Roberts, K.; Walter, P. *Molecular Biology of the Cell*, 5th ed.; Garland Science: New York, 2007.

(2) Howard, J. *Mechanics of Motor Proteins and the Cytoskeleton*; Sinauer Associates: Sunderland, MA, 2001.

(3) Bray, D. *Cell Movements: From Molecules to Motility*; 2-nd ed.; Garland Publishing: New York, 2001.

(4) Desai A.; Mitchison T.J. Microtubule Polymerization Dynamics. *Annu. Rev. Cell Dev. Biol.* **1997**, *13*, 87-117.

(5) Gardner, M.K.; Zanic, M.; Howard, J. Microtubule Catastrophe and Rescue. *Curr. Opin. Cell Biol.* **2013**, *25*, 14-22.

(6) Kerssemakers, J.W.J.; Munteanu, E.L.; Laan, L.; Noetzel, T. L.; Janson, M. E.; Dogterom, M. Assembly Dynamics of Microtubules at Molecular Resolution. *Nature* **2006**, *442*, 709-712.

(7) Schek H.T.; Hunt A. Microtubule Assembly Dynamics at the Nanoscale. *Curr. Biol.* **2007**, *17*, 1445-1455.

(8) Mitchison T.; Kirschner M. Dynamic Instability of Microtubule Growth. *Nature* **1984**, *312*, 237-242.

(9) Brun, L.; Rupp, B.; Ward, J.J.; Nedelec, F. A Theory of Microtubule Catastrophes and their Regulation. *Proc. Natl. Acad. Sci. USA.* **2009**, *106*, 21173-21178.

(10) Dimitrov, A.; Quesnoit, M.; Moutel, S.; Cantaloube, I.; Pous, C.; Perez, F. Detection of GTP-Tubulin Conformation in Vivo Reveals a Role for GTP Remnants in Microtubule Rescues. *Science* **2008**, *322*, 1353-1356.

(11) Odde, D.J.; Cassimeris, L.; Buettner, H.M. Kinetics of Microtubule Catastrophe Assessed by Probabilistic Analysis. *Biophys. J.* **1995**, *69*, 796-802.

(12) Stepanova, T; Smal, I; van Haren, J; Akinci, U; Liu, Z; Miedema, M; Limpens, R; van Ham, M; van der Reijden, M; Poot, R., et al. History-Dependent Catastrophes Regulate Axonal Microtubule Behavior. *Curr. Biol.* **2010**, *20*, 1023-1028.

(13) Drechsel, D.N.; Hyman, A.A.; Cobb, M.H.; Kirschner, M.W. Modulation of the Dynamic Instability of Tubulin Assembly by the Microtubule-Associated Protein Tau. *Mol. Biol. Cell* **1992**, *3*, 1141-1154.

(14) Flyvbjerg, H.; Holy, T.E.; Leibler, S. Stochastic Dynamics of Microtubules: A Model for Caps and Catastrophes. *Phys. Rev. Lett* **1994**, *73*, 2372-2375.

(15) Li, X.; Kolomeisky, A.B. Theoretical Analysis of Microtubules Dynamics Using a Physical-Chemical Description of Hydrolysis. *J. Phys. Chem. B* **2013**, *117*, 9217-9223.

(16) Li, X.; Kolomeisky, A.B. A New Theoretical Approach to Analyze Complex Processes in Cytoskeleton Proteins. *J. Phys. Chem. B* **2014**, *118*, 2966-2972.

(17) Kueh, H.Y.; Brieher, W.M.; Mitchison, T.J. Dynamic Stabilization of Actin Filaments. *Proc. Natl. Acad. Sci. USA.* **2008**, *105*, 16531-16536.

(18) Li, X.; Kierfeld, J.; Lipowsky, R. Actin Polymerization and Depolymerization Coupled to Cooperative Hydrolysis. *Phys. Rev. Lett.* **2009**, *103*, 048102.

(19) Gardner, M.K.; Zanic, M.; Gell, C.; Bormuth, V.; Howard, J. Depolymerizing Kinesins Kip3 and MCAK Shape Cellular Microtubule Architecture by Differential Control of Catastrophe. *Cell* **2011**, *147*, 1092-1103.

(20) Coombes, C.E; Yamamoto, A.; Kenzie, M.R.; Odde, D.J.; Gardner, M.K. Evolving Tip Structures Can Explain Age-Dependent Microtubule Catastrophe. *Curr. Biol.* **2013**, *23*, 1342-1348.

(21) Padinhateeri, R.; Kolomeisky, A. B.; Lacoste, D. Random Hydrolysis Controls the Dynamic Instability of Microtubules. *Biophys. J.* **2012**, *102*, 1274-1283.

(22) Pantaloni, D.; Hill, T.L.; Carlier, M.F.; Korn, E.D. A Model for Actin Polymerization and the Kinetic Effects of ATP Hydrolysis. *Proc. Natl. Acad. Sci. USA.* **1985**, *82*, 7207-7211.

(23) Vavylonis, D.; Yang, Q.; O'Shaughnessy, B. Actin Polymerization Kinetics, Cap Structure, and Fluctuations. *Proc. Natl. Acad. Sci. USA.* **2005**, *102*, 8543-8548.

(24) Stukalin, E.B.; Kolomeisky, A. B. ATP Hydrolysis Stimulates Large Length Fluctuations in Single Actin Filaments. *Biophys. J.* **2006**, *90*, 2673-2685.

(25) Blanchoin, L.; Pollard, T. D. Hydrolysis of ATP by Polymerized Actin Depends on the Bound Divalent Cation but Not Profilin. *Biochemistry* **2002**, *41*, 597-602.

(26) VanBuren, V.; Odde, D. J.; Cassimeris, L. Estimates of Lateral and Longitudinal Bond Energies within the Microtubule Lattice. *Proc. Natl. Acad. Sci. USA.*, **2002** *99*, 6035-6040.

(27) Pieper, U.; Wegner, A. The End of a Polymerizing Actin Filament Contains Numerous ATP-Subunit Segments That Are Disconnected by ADP-Subunits Resulting from ATP Hydrolysis. *Biochemistry* **1996**, *35*, 4396-4402.

(28) Antal, T.; Krapivsky, P. L.; Redner, S.; Mailman, M.; Chakraborty, B. Dynamics of an Idealized Model of Microtubule Growth and Catastrophe. *Phys. Rev. E* **2007**, *76*, 041907.

(29) Li X.; Lipowsky R.; Kierfeld J. Coupling of Actin Hydrolysis and Polymerization: Reduced Description with Two Nucleotide States. *Europhys. Lett* **2010**, *89*, 38010.

(30) Burnett, M. M.; Carlsson, A. E. Quantitative Analysis of Approaches to Measure Cooperative Phosphate Release in Polymerized Actin *Biophys. J.* **2012**, *103*, 2369-2378.

(31) Janson, M.E.; de Dood, M.E.; Dogterom, M. Dynamic Instability of Microtubules Is Regulated by Force. *J. Cell Biol.* **2003**, *161*, 1029-1034.

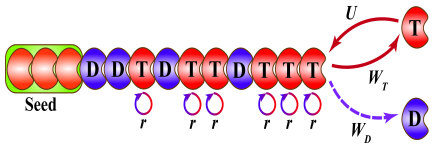

Figure 0: TOC